

Magneto optical rib waveguide with low refractive index

A. Bouchelaghem¹, A. Hocini^{1,2,*}, D. Saigaa¹, T. Bouchemat², F. Royer³ and J.J. Rousseau³

¹ *Département d'Electronique, Faculté de Technologie Université de M'sila, Algeria.*

² *Laboratoire Micro système et Instrumentation, Université Mentouri Constantine, Algeria.*

³ *Laboratoire Telecom Claude Chappé (LT2C)A 3523, Université Jean Monnet, 25, rue du Dr Rémy ANNINO 42000*

St Etienne Cedex 2, France

** hocini74@yahoo.fr*

Abstract: The phase matching condition is an important requirement for magneto-optical waveguide devices. In this work, the design rules that must be imposed on the geometry and the index of magneto optical rib waveguides to make them behave as phase matched rib waveguides have been simulated. Using film mode matching method, the results show that operation in phase matching is possible under certain circumstances with selected index and geometries. We simulated the performance of such devices and we determined the waveguide dimensions (height, width, and etching depth) and the index that satisfy the phase matching conditions.

Keywords: Integrated optics; Magneto-optic; Rib waveguides; birefringence.

I. Introduction

Magneto-optic waveguides are the basic elements for non-reciprocal integrated optics and the phase matching between the fundamental TE and TM modes is an essential condition in magneto-optic waveguides. This condition can be satisfied with selected geometries rib waveguides.

More and more, the sol-gel process gives a solution to fabricate integrated optic devices. It is considered as a versatile, flexible and a low-cost technique useful for the realization of integrated photonic devices[1]. Many functions are needed in optical processing to be integrated. Among these functions are optical waveguide isolators that have a nonreciprocal effect and are very important in optical network systems.

Currently, only bulk forms of these components, made of garnet oxide crystals, are commercially available, and integrated versions are highly desirable. The use of magnetic nanoparticles, as magneto-optical active element in a silica-based matrix prepared via sol-gel process, has been discussed in a large number of papers from first of these [3] to the most recent [4]. This latter is prepared via organic-inorganic process. The attraction of such approach lies in the full compatibility of the sol-gel coating with classical integrated technologies and especially the technology on glass. Indeed, crystallized magnetic nanoparticles are dispersed in the sol-gel liquid preparation before the coating and, thus, contrarily to classical techniques, high temperature is not required to obtain a magnetic behavior. Furthermore, this elaboration method is easy to implement and provide magneto-optical thin films with a refractive index value (1.5) close to that of other integrated optical devices. The inherent low refractive index contrast between the film

and the substrate in sol-gel organic inorganic waveguides combined with a thickness larger than that of classical magneto-optical waveguides should allow an efficient fiber coupling which is highly desirable for laser-waveguide coupling [2, 4].

The phase matching between the fundamental TE and TM modes is an essential condition in magneto-optic waveguides. The problem of thin-film phase mismatch between TE and TM modes

($\Delta\beta = \beta_{TE} - \beta_{TM} = 2\pi\Delta N_m/\lambda$, ΔN_m is the modal birefringence) affects with Faraday rotation the conversion efficiency in these films which is expressed as [2]:

$$R = \frac{\theta_F^2}{\theta_F^2 + (\Delta\beta/2)^2} \quad (1)$$

θ_F (°/cm) is the specific Faraday rotation of the material constituting the waveguide.

The present work describes the design rule that must be imposed to the geometry and the refractive index of such device to make them behave as phase-matched rib waveguides. It consists of the tuning of the geometrical parameters and the contrast of the film ; see Fig. 1.

In order to design a waveguide with zero-birefringence, the first step was to investigate the polarization characteristics of the rib waveguide due to its geometry. The software, based on the film mode matching (FMM) method [4], all the modes propagating in the rib waveguide are calculated for both TE and TM polarizations and the corresponding effective index (n_{eff}) and propagation constant β are determined. To

obtain zero-birefringence in rib waveguide, an optimization of waveguide dimensions is necessary.

II. Device modelling

The device design has been carried out with vectorial 3D-mode solver FIMMWAVE (Photon Design) [7] the device is shown schematically in fig 1. Where W is the rib width, H is the inner rib height, r is the fractional height of the side regions compared to the rib center (the outer-inner ratio) as defined in Fig. 1. For a better understanding, we will also consider the etching depth $D = H(1-r)$ which directly gives the edge height of the rib waveguide.

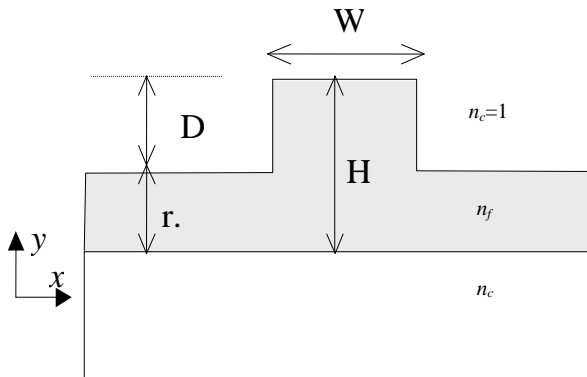


Fig.1. Schematic representation of a Rib waveguide. Structural parameters are the height h and the width w and refractive-index n_s , n_f .

We have chosen waveguide optical parameters corresponding to SiO₂/ZrO₂ film or SiO₂/TiO₂ doped with magnetic and by adjusting the molar ratio of metallic precursors, that the refractive index can be varied in range 1.51 to 1.58 at $\lambda = 1550$ nm on PyrexTM substrate ($n_s = 1.472$; $\lambda = 632.8$ nm) [5].

Tuning of $\Delta\beta$ by varying the refractive index of the film to obtain phase matching condition, we chose the two values of refractive index $n = 1.51$ and 1.57 .

III. Numerical Simulations

The initial height are set to $3 \mu\text{m}$. Using FIMMWAVE, the effective indices of the fundamental TE and TM waveguide modes were monitored as the width and the etch depth were varied, at $\lambda = 1.55 \mu\text{m}$.

The iteration of the simulation was repeated for a given values of the parameter r . Hence, the process is one in which we determine the effective indices of the fundamental TE and TM waveguide modes as the waveguide width is gradually increased, and a series of ΔN points were calculated.

Figure 2 and Figure 3 show a plot of the birefringence as a function of the width for different etch depth for $n = 1.51$ and 1.57 respectively, for different parameter r , the results show that for smaller values of etch depths the birefringence is always positive, the fundamental quasi-TE and quasi-TM waveguide modes cannot be equalized

by varying values of waveguide width. And as the parameter r decreases, a tendency for two specific values of waveguide widths for which the effective index of the fundamental quasi-TE and quasi-TM waveguide modes can be equalized. The intersection of the curves with the axe zero indicates that both TE and TM polarizations have the same effective index and therefore the waveguide is phase matched in terms of propagation constant.

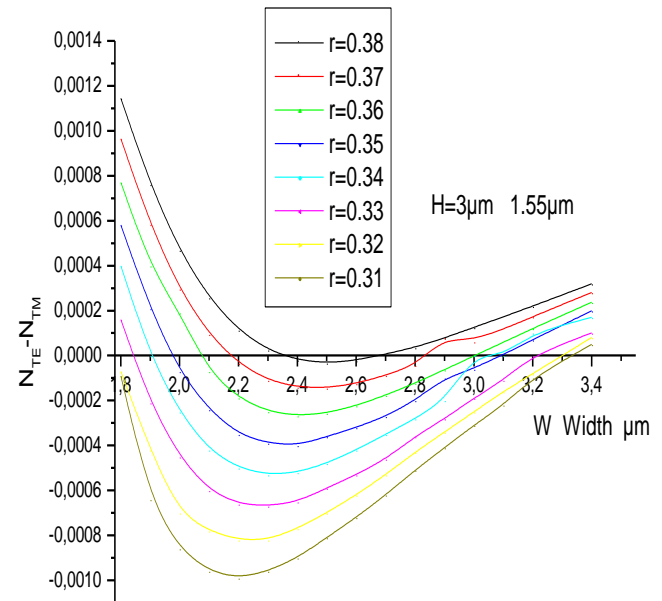


Fig.2. Birefringence calculation between TE and TM modes for $n = 1.51$ at $\lambda = 1.55 \mu\text{m}$.

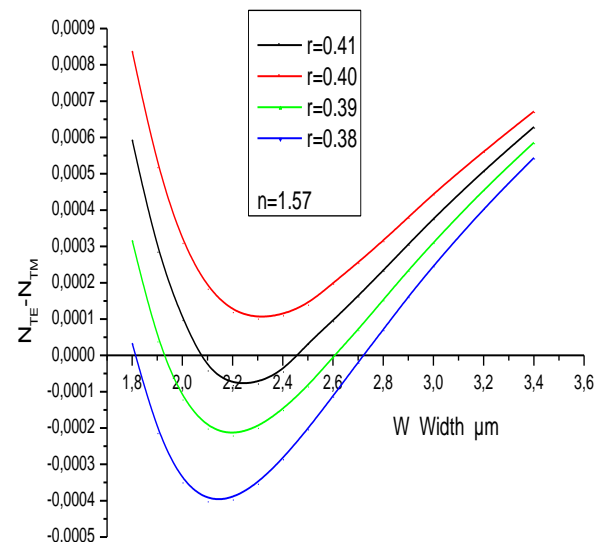


Fig.3. Birefringence calculation between TE and TM modes for $n = 1.57$ at $\lambda = 1.55 \mu\text{m}$.

The intersections of the two curves with axe of zero-birefringence are used to study the variation of the

parameter r as function of the width W in order to obtain phase matching condition. Figure 4 shows clearly that the parameter r , corresponding to the phase matching condition, increases (or etch depth D decreases) according to the decrease of the refractive index. The maximum of r (corresponding to minimum of etching depth) is observed for the two curves, and the calculated points are fitted by polynomial of degree 2.

We note that there is a maximum parameter r_{\max} (minimum etch depth) D_{\min} for each waveguide design of $n_1=1.51$ and $n_2=1.57$ $r_{\max 1} = 0.38$ $r_{\max 2} = 0.40$, respectively. The parameter r (etching depth D) is the more critical parameter for the fabrication of such waveguides

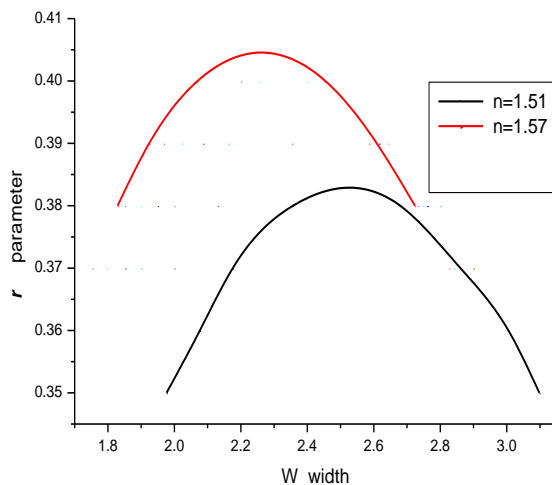


Fig.4. Waveguide width influence on parameter r in the structure to support zero birefringence for waveguide index $n=1.51$ and 1.57 at $\lambda=1.55\mu\text{m}$

The field distribution in the rib waveguide for the TE and TM polarizations is shown in Fig. 5 for the two minimum etch depth (r_{\max}). The TE field slightly expands in the film region, and this effect is more important as the refractive index is increased. The TM mode appears to be better confined in the central part of the rib waveguide.

Increasing the waveguide width yields more similar field profiles of the TE and TM modes in the guide. This behavior can be explained by the fact that effective index increases with the width, implying a stronger confinement.

IV. Conclusion

An analysis of the modal birefringence in magneto optical Thin Film has been presented, using mode solver program to provide theoretical prediction that certain waveguide geometries can lead to zero-birefringence, the etching depth, width, height and refractive index values have been determined to design waveguides with zero-birefringence condition, for $1.55\mu\text{m}$

In the rib waveguide, it has been shown that the zero-birefringence condition is valid only for deeply etched waveguides. We have found that there are more choices for waveguide with great value of index at $\lambda=1550\text{nm}$.

In the future, such structure can find a wide application in optoelectronic devices, and that may be interesting to realize waveguides made of magnetophotonic crystals.

Acknowledgment

The authors wish to thank l'Agence Nationale pour le Développement de la Recherche Universitaire (ANDRU) Algeria.

References

- [1] A. Chiappini, C. Armellini, A. Chiasera, M. Ferrari, R. Guider, Y. Jestin, L. Minati, E. Moser, G. Nunzi Conti, S. Pelli, [2] R. Retoux, G.C. Righini, G. Speranza, Journal of Non-Crystalline Solids. 355, 1132–1135(2009)
- [3] F. Royer, D. Jamon, and J. J. Rousseau, H. Roux, D. Zins and V. Cabuil. Applied Physics letters. 86, 011107 (2005)
- [4] M.F. Bentivegna, M. Nyvlt, J. Ferre, J.P. Jamet, A. Brun, S. Visnovsky, R. Urban, J. Appl. Phys. 58, 2270(1999)
- [5] F. Choueikani, et al. Applied Physics letters. 94, 051113(2009)
- [6] V. Zayets, M. C. Debnath, and K. Ando, Appl. Phys. Lett. 84, 565 (2004)
- [7] A. Sv. Sudbø, IEEE Photon. Technol. Lett. 5, 342 (1993)
- [8] FIMMWAVE program, Photon Design Product [http://www.photond.com]
- [9] A. Hocini et al, Applied Physics B: Lasers and Optics. 99, no. 3, (May 2010): 553 -558.